International Immunopharmacology 70 (2019) 241–251

Contents lists available at ScienceDirect

International Immunopharmacology

journal homepage: www.elsevier.com/locate/intimp

Application of highly efficient and lowly toxic bufadienolides screened from toad skin in lymphatic chemotherapy for colorectal cancer through a lymphatic metastatic model

Changzheng He[a,1], Zhenyu Zou[b,1], Shaoyou Xia[a,1], Xiaowei Xing[a,1], Shidong Hu[a], Zilong Hu[c], Yuxuan Li[a], Songyan Li[a], Hongliang Zhang[a], Yu Yang[a], Yichen Liu[a], Xiaolei Xu[a], Boyan Liu[a], Yufeng Wang[d], Yingxin Xu[e,*], Xiaohui Du[a,**]

[a] Department of General Surgery, Chinese General Hospital of People's Liberation Army, Beijing 100853, PR China
[b] Department of Hernia and Abdominal Wall Surgery, Beijing Chaoyang Hospital, Capital Medical University, Beijing 100043, PR China
[c] Department of General Surgery, Beijing Chaoyang Hospital, Capital Medical University, Beijing 100020, PR China
[d] Department of Patient Admission Management, Chinese General Hospital of People's Liberation Army, Beijing 100853, PR China
[e] Institute of General Surgery, Chinese General Hospital of People's Liberation Army, Beijing 100853, PR China

ARTICLE INFO

Keywords:
Bufadienolides
Colorectal cancer
Emulsion
Lymph node metastasis
Lymphatic chemotherapy

ABSTRACT

Background: Lymph node metastasis (LNM) remains a major obstacle to treat colorectal cancer (CRC). Increasing evidences have suggested that bufadienolides contain several fractions displaying antitumor activity and may be applied in lymphatic chemotherapy. However, effects of the highly efficient and lowly toxic (HELT) bufadienolides on CRC in lymphatic chemotherapy have not been reported.

Methods: Adenosine triphosphate tumor chemosensitivity assays (ATP-TCA) was performed to detect the inhibition rate (IR) of fractions of bufadienolides to cytokine-induced killer (CIK) cells and tumor cells. HELT fraction-loaded emulsions of different concentrations were prepared. Nude mouse bearing HCT116 tumors in footpad received high-dose emulsion (HD-E), middle-dose emulsion (MD-E), low-dose emulsion (LD-E), control emulsion (CE), Cinobufacini Injection (CI), or normal saline (NS), respectively. Hematoxylin and eosin (H&E) staining, Flow Cytometry (FCM), enzyme-linked immune sorbent assay (ELISA) and hematological examination were applied to evaluate therapeutic effects and potential toxicity.

Results: F18 and F19 were screened out as HELT fractions *in vivo* and F18-loaded emulsions of different concentrations for lymphatic administration were prepared. We confirmed that HD-E and MD-E produced obvious antitumor activities in footpad tumors and LNM compared with other groups *in vitro*. We also verified the effects of F18-loaded emulsions on activating hematopoietic function, stimulating proliferation of the spleen and natural killer (NK) cells, and promoting the secretion of IFN-γ and IgG1, although HD-E performed mild toxicity on liver.

Conclusion: The present study demonstrated that lymphatic chemotherapy with HELT fraction of bufadienolides could be an effective approach to the treatment of CRC patients with LNM.

1. Introduction

Colorectal cancer (CRC) is the third most common cancer and the second leading cause of cancer death according to GLOBOCAN 2018 [1]. Lymph node metastasis (LNM) is one of the determinant prognostic factors of CRC [2]. Unfortunately, conventional intravenous chemotherapeutics are difficult to highly concentrate in regional lymph nodes on account of the anatomical properties of lymphatic system, which results in limited therapeutic effects. Furthermore, the chemotherapeutics rapidly accumulating in normal organs and tissues could inevitably cause severe side effects [3]. Therefore, lymphatic chemotherapy may solve these problems by distributing more drugs in lymphatic system and less in blood circulation.

Currently, lymphatic chemotherapy has been proved to have

* Correspondence to: Y. Xu, Institute of General Surgery, Chinese General Hospital of People's Liberation Army, No. 28 Fuxing Road, Beijing 100853, PR China.
** Correspondence to: X. Du, Department of General Surgery, Chinese General Hospital of People's Liberation Army, No. 28 Fuxing Road, Beijing 100853, PR China.
E-mail addresses: xuyingx@126.com (Y. Xu), duxiaohui301@sina.com (X. Du).
[1] These authors contributed equally to this work.

https://doi.org/10.1016/j.intimp.2019.02.036
Received 8 January 2019; Received in revised form 14 February 2019; Accepted 22 February 2019
Available online 06 March 2019

satisfactory antitumor effects on various cancers [4–8]. Previous studies showed that using several drug-loaded carriers [8–12] to absorb or encapsulate chemotherapeutics provided a better penetration into lymphatics. However, the lymphatic uptake rate is not high and the biocompatibility of some carrier materials is not ideal for the lymphatic system, which may lead to some adverse reactions [13]. Currently, drugs rather than drug carriers that being appropriate to lymphatic chemotherapy are needed. At this point, traditional Chinese medicine (TCM) possesses obvious advantages [14]. Bufadienolides, the major active components of the skin of *Bufo bufo gargarizans* Cantor (toad skin) have shown high antitumor activities and also a broad spectrum to various cancer cell lines, such as human astrocytoma, lung and gastric tumors [15]. However, they also performed high toxicity or serious side effects clinically [16]. Fractions of bufadienolides such as resibufogenin have the antitumor effect as well as toxicity and other side effects [17,18]. Thus, it is essential to identify the fractions of bufadienolides with high antitumor activity and low toxicity for application in lymphatic chemotherapy, in order to decrease cytotoxicity to the greatest extent.

In the present study, the effects of 22 fractions of bufadienolides on tumor cells and cytokine-induced killer (CIK) cells were evaluated and two fractions (F18 and F19) with high efficiency and low toxicity (HELT) were screened. The anticancer efficacy, the effects on immune function, and the potential toxicity of F18 in lymphatic chemotherapy were assessed in a CRC model with lymphatic metastasis.

2. Materials and methods

2.1. Preparation of bufadienolides and standard solution

Bufadienolides separated and purified from the skin of *Bufo bufo gargarizans* Cantor (toad skin) have been previously described in detail [19]. Briefly, 4 kg dried toad skin was decocted with 95% ethanol. The combined decoctions were dried with rotary evaporation at 60 °C in vacuum. 140 g extract was dissolved in 70% methanol again, and then extracted with n-heptane. Methanol fraction was dried and 40 g residue was dissolved in methanol and filtered through 0.45 μm membrane filter to form the sample of 440 mg/mL. After that, the crude sample was fractionated with preparative high-performance liquid chromatography (prep-HPLC) and 22 fractions (labeled as F1–F22) were collected according to the absorption peaks. Finally, the fractions were purified on the water purification factory. Dr. Xiuli Zhang and Prof. Xinmiao Liang from Dalian Institute of Chemical Physics, China Academy of Science (Dalian, China) provided these 22 fractions for further study about pharmacological activities and toxicity in our laboratory. All fractions were stored at −20 °C.

Every fraction was weighted and completely dissolved with dimethyl sulfoxide (DMSO; Sigma, St. Louis, MO, USA) at the solubility of 200 mg/mL, and then diluted to the final concentrations of 2, 0.5, and 0.1 μg/mL with adenosine triphosphate tumor chemosensitivity assays (ATP-TCA) kit cell culture medium (Jinzijing Biotech Co. Ltd., Beijing, China) and Cellix 601 serum-free medium (SIMA, Beijing, China), respectively. To avoid affecting cell activity, we kept DMSO concentration < 0.1% (v/v). All solutions were filtered through 0.22 μm membrane filter (Pall, USA), stored at 4 °C, and brought to room temperature before use.

2.2. Cell culture

The human colorectal adenocarcinoma cell line HCT116 was obtained from the Tumor Epigenetics and Early Detection Laboratory, Chinese People's Liberation Army (PLA) General Hospital (Beijing, China) and cultured in RPMI-1640 medium (Sigma) supplemented with 10% heat-inactivated fetal bovine serum (FBS; Gibco Inc.), 50 U/mL penicillin, and 50 mg/mL streptomycin at 37 °C with 5% CO_2. The human gastric adenocarcinoma cell line BGC823 and human pancreatic carcinoma cell line SW1990 were obtained from the Institute of General Surgery, Chinese PLA General Hospital (Beijing, China) and cultured in Dulbecco's Modified Eagle Medium (DMEM; Sigma) with 10% heat-inactivated FBS and 1 U/mL gentamicin at 37 °C with 5% CO_2. Cells in the logarithmic phase of growth were collected for the experiment.

CIK cells were isolated and cultured as described previously [20,21]. Briefly, 50 mL of peripheral blood from healthy adult donors was drawn. Participants in our study all provided written informed consents. Peripheral blood mononuclear cells (PBMCs) were isolated by density gradient Ficoll-Paque centrifugation (TBD, Tianjin, China), washed with saline, and then cultured in Cellix 601 serum-free medium (SIMA) for 3 h. To prepare CIK cells, the non-adherent cells were harvested, stimulated with 1000 U/mL recombinant interferon (IFN)-γ (SIMA) in Cellix 601 serum-free medium (SIMA, Beijing, China) at 37 °C with 5% CO_2 for 24 h, and then activated with 20 μg/mL anti-CD3, 1 μg/mL anti-CD28 (Mabworks Biotech, Beijing, China), and 1000 U/mL recombinant IL-2 for 12–14 days.

2.3. Co-culture and microscopy

To evaluate the effects of 22 fractions on different tumor cells and CIK cells, 2×10^3 tumor cells and 2×10^4 CIK cells were seeded into each well of a 96-well polypropylene microplate (Costar, USA), respectively. The standard solutions of 22 fractions were added in triplicate at three different final concentrations of 2, 0.5, and 0.1 μg/mL. The plates were incubated for 72 h at 37 °C with 5% CO_2. The cells were observed microscopically to check for overgrowth, and photographed by TE2000-U inverted microscope (Nikon, Japan) after 24, 48, and 72 h of co-culture.

2.4. ATP-TCA chemosensitivity assay

At the end of the 72-h incubation period, chemosensitivity was assessed using the ATP-TCA kit (Jinzijing Biotech Co. Ltd., Beijing, China). Briefly, remaining cells were lysed by the addition of 50 μL of tumor cell extraction reagent (trichloroacetic acid; Jinzijing Biotech). 50 μL of the lysate from each well was added to corresponding wells in a white 96-well microplate (Jinzijing Biotech) followed by the addition of 50 μL of luciferin-luciferase reagent (Jinzijing Biotech). The level of ATP present was measured on the basis of the absorbance (A) values at 562 nm using a BHP9504 Luminometer (Hamamatsu Photon Techniques Inc., Beijing, China). Luminescence measurements are directly related to ATP levels and enable to determine the percentage of living cells. The cell growth inhibition rate (IR) was calculated using the following equation: IR = (1 − experimental group A value / control group A value) × 100%. Three categories of *in vitro* sensitivity were defined as: (a) strong sensitivity (SS), IR ≥ 70%; (b) partial sensitivity (PS), 50 ≤ IR < 70%; (c) resistance (R), IR < 50%. Thus, IR ≥ 70% to tumor cells was defined as high efficiency and IR < 50% to CIK cells was defined as low toxicity.

2.5. Preparation of emulsion

Emulsion has lymphatic affinity and also characteristic of coating drugs in the internal phase, for which drugs can be protected from hydrolysis and be improved of clinical efficacy [22]. Furthermore, previous studies have shown that lymphatic targeting of water in oil (W/O) emulsions after local injection is better than that of oil in water (O/W) emulsions [23]. Thus, the W/O emulsions with various concentrations of HELT fractions were prepared following the previous methods [24]. Briefly, to obtain the oil phase, 0.3 g Oleum Camelliae (Jinhaitang Medicinal Oil Co. Ltd., Jiangxi, China) and 0.1 g soybean lecithin (Sigma) were added into appropriate amount of ethanol and warmed up to 60 °C in the water bath. To obtain the water phase, F18 (25 mg for high-dose emulsion, 2.5 mg for middle-dose emulsion, and 0.5 mg for low-dose emulsion) dissolved in DMSO, 0.2 g poloxamer

(Sigma), 1.5 g glycerol (Chemworks, Beijing, China), 1.5 g propylene glycol (Xilong Chemical Co. Ltd., Guangxi, China), and sterile water were churned and heated to 60 °C. The water phase was added slowly into the oil phase and expanded to 10 mL with sterile water to form the colostrum. Then, the colostrum was shaken with a DS-5510DT ultrasonic instrument (Shengxi, Ultrasound equipment Ltd., Shanghai, China) for 10 min to form the emulsion. The concentrations of high-dose, middle-dose, and low-dose emulsions were 2.5, 0.25, and 0.05 mg/mL, respectively. All emulsions filtered through 0.22 μm membrane filter and stored at 4 °C.

2.6. Establishment of LNM models

The experimental protocol was approved by the ethics review committee for animal experimentation at our institution. All experimental mice were raised in special pathogen free (SPF) condition in the Experimental Animal Center of PLA 302 Hospital (Beijing, China). Six-week-old female BALB/c nude mice were anesthetized by ether inhalation anesthesia and then placed in a supine position. The human CRC lymphatic metastasis model of the nude mouse was established by injecting 4×10^6 HCT116 cells at a total volume of 40 μL subcutaneously into the right hind footpad, similar to previous reports [25,26].

2.7. Effect of HELT fraction emulsions on in situ tumor and lymph metastasis

Cinobufacini Injection (CI) is an aqueous extraction from toad skin, which is now widely used in clinical therapy for various cancers, arrhythmia, and heart diseases in China. In the present study, we took CI as a positive control. At the 3rd day of injection, 48 tumor-bearing nude mice were randomized into 6 groups and treated with normal saline (NS) (blank control), control emulsion (CE) containing 1.25% (v/v) DMSO, CI (0.4 mL/kg equals clinical therapeutically dose: intravenous injection of 20 mL/50 kg per day for adults, equivalent to 0.5 g/mL of herbal pieces prepared for decoction; Jinchan Biotech, Anhui, China), F18 high-dose emulsion (HD-E; 5 mg/kg), F18 middle-dose emulsion (MD-E; 0.5 mg/kg), and F18 low-dose emulsion (LD-E; 0.1 mg/kg). Each group underwent footpad peritumoral injection (lymphatic chemotherapy) at a dosage of 0.04 mL/20 g for 18 days. The gross tumor volume was calculated according to the following equation: V (mm^3) = (length × $width^2$) / 2. After treatment, the mice were killed. The footpad tumors, subiliac lymph nodes, medial iliac lymph nodes, and renal lymph nodes were dissected and observed by hematoxylin and eosin (H&E) staining. The tumor inhibition rate (IR) and LNM rate were respectively calculated according to the following equations: IR = [1 − tumor weight (experimental) / tumor weight (control)] × 100%; LNM rate = [1 − number (metastatic) / number (detected)] × 100%.

2.8. Effect of HELT fraction emulsions on immune function

The spleen is an important immune organ, and the spleen index (SI) can reflect the immune state to a certain extent. Thus, the spleen was removed after treatment and the SI value was calculated by (spleen weight / body weight) × 10. Then spleen cells were cultured according to the standard procedures. Since the lack of thymus and the loss of T cell immunity, natural killer (NK) cells and B cells become the main force of antitumor immunity in nude mice. The activated NK cells secrete IFN-γ while effector B cells synthetizes and secretes antibodies. Thus, we respectively analyzed the proportion of NK cells among peripheral blood and spleen by Flow Cytometry (FCM). In addition, we respectively detected the content of IFN-γ and IgG1 in serum as well as the splenic cell supernatant by enzyme-linked immune sorbent assay (ELISA) according to the manufacturer's instructions.

2.9. Evaluation of the potential toxicity

Potential toxicity treated with HELT faction emulsions at different concentrations has been investigated. Gross measures such as weight loss, behavior and feeding were evaluated. The blood was drawn after treatment and the biochemical indexes of blood and liver were analyzed.

2.10. Statistical analysis

Data were expressed as the mean ± SD. Differences between groups were analyzed by one-way analysis of variance (ANOVA) and Student *t*-test using the SPSS 20.0 statistical software (SPSS Inc., Chicago, IL, USA). $P < 0.05$ was considered to indicate a statistically significant difference.

3. Results

3.1. Physical property and effects on cell growth of fractions of bufadienolides

The physical property of 22 fractions of bufadienolides was shown in Table 1. F1–F5 were water-soluble. F6–F22 were soluble in DMSO, an effective solvent for a wide array of organic materials.

The effects of these 22 fractions on three different tumor cells of digestive system and CIK cells were observed by microscope. Four categories of fractions were divided: (a) fractions promoted growth of tumor cells and CIK cells, namely F1; (b) fractions inhibited growth of tumor cells and CIK cells, namely F4–F17; (c) fractions inhibited growth of tumor cells but not obviously inhibited growth of CIK cells, namely F18 and F19; (d) unstable fractions susceptible to concentration, namely F2–3 and F20–22. Representative photomicrographs of each category from HCT116, BGC823, SW1990 and CIK cells co-cultured with three concentrations of 22 fractions were shown in Fig. 1.

3.2. Screening of HELT fractions of bufadienolides

Based on *in vitro* ATP-TCA experiments, the cell growth inhibition by 22 fractions was examined. As the definition we described previously, fractions whose IR ≥ 70% to tumor cells and IR < 50% to CIK cells were considered as HELT fraction. The results indicated that cell growth inhibition of each fraction on tumor cells and CIK cells were

Table 1
Physical property of fractions from bufadienolides.

Fraction	Color	Property	Solubility
1	Brown	Meliceris	Water-solubility
2	Puce	Meliceris	Water-solubility
3	Brown	Meliceris	Water-solubility
4	Brown	Granular	Water-solubility
5	Brown	Granular	Water-solubility
6	Beige	Granular	Liposolubility
7	Beige	Granular	Liposolubility
8	Beige	Granular	Liposolubility
9	Brown	Granular	Liposolubility
10	Beige	Granular	Liposolubility
11	Beige	Granular	Liposolubility
12	Brown	Meliceris	Liposolubility
13	Beige	Granular	Liposolubility
14	Beige	Granular	Liposolubility
15	Ecru	Powder	Liposolubility
16	Brown	Meliceris	Liposolubility
17	Brown	Granular	Liposolubility
18	Puce	Meliceris	Liposolubility
19	Puce	Meliceris	Liposolubility
20	Puce	Meliceris	Liposolubility
21	Puce	Meliceris	Liposolubility
22	Puce	Meliceris	Liposolubility

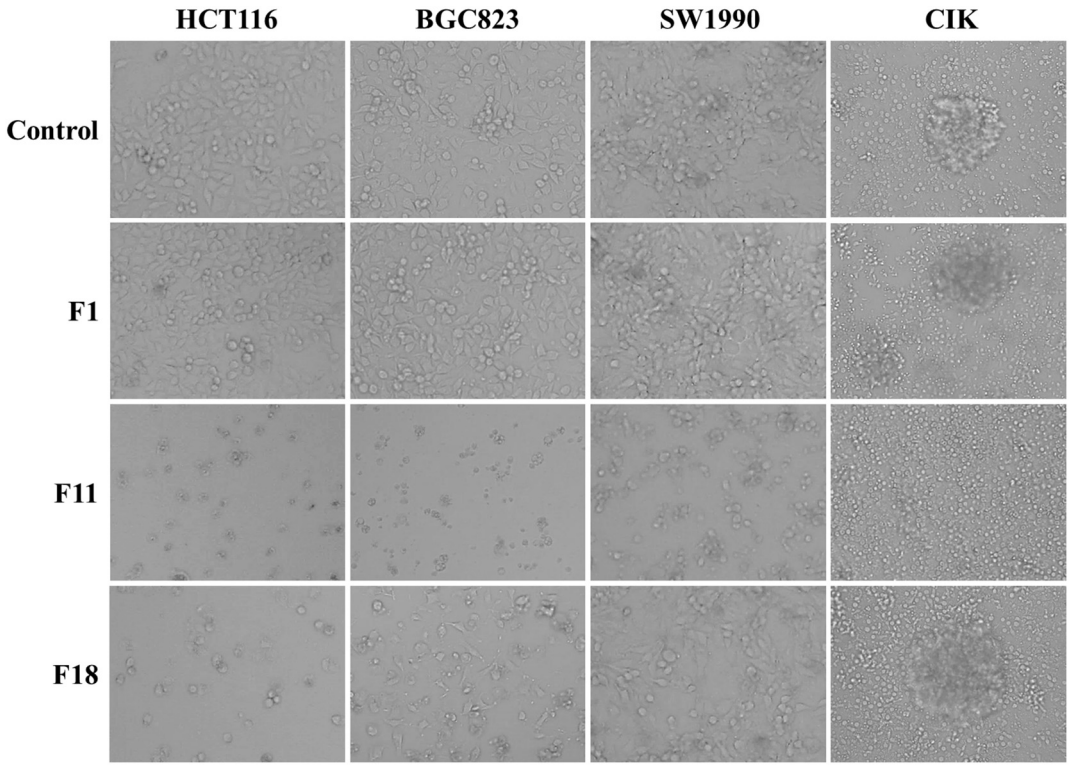

Fig. 1. Representative photomicrographs were obtained from HCT116, BGC823, SW1990, and CIK cells co-cultured respectively with F1, F11, and F18 at concentration of 0.5 μg/ml for 3 days. Original magnification, ×100 for tumor cells, ×200 for CIK cells.

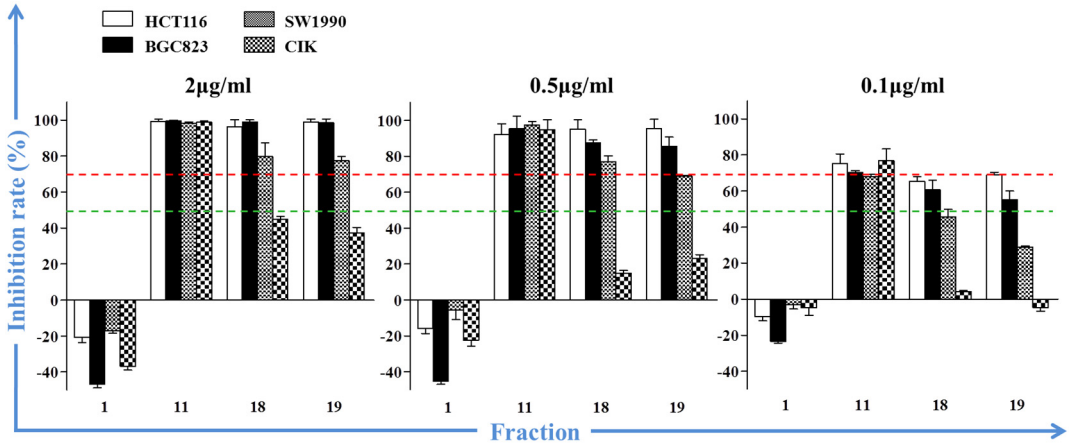

Fig. 2. Assessment of the *in vitro* cell growth inhibition of treatment with representative factions. HCT116, BGC823, SW1990, and CIK cells were respectively treated with F1, F11, F18, and F19 at concentrations of 2, 0.5, and 0.1 μg/mL for 3 days. The cell growth inhibition rate was evaluated by ATP-TCA. The data are presented as the mean ± SD of three independent experiments. The red dashed line represents IR = 70%. The green dashed line represents IR = 50%. Negative value illustrates a promoter action to cells. (For interpretation of the references to color in this figure legend, the reader is referred to the web version of this article.)

reduced with the reduction of concentration. In addition, the four categories of fractions observed by microscope were proved by ATP-TCA (Fig. 2). Among these 22 fractions, F1 promoted the growth of tumor cells and CIK cells. F11 intensively inhibited the growth of tumor cells and CIK cells. These two categories and the unstable fractions were undesirable in antitumor research. However, the other categories that inhibited growth of tumor cells but not obviously inhibited growth of CIK cells met the requirements of antitumor treatments. Specifically, at concentration of 2 μg/mL, IRs of F18 were 96.24 ± 3.92% to HCT116 cells, 98.84 ± 1.28% to BGC823 cells, 79.67 ± 7.65% to SW1990 cells, and 45.00 ± 1.48% to CIK cells; IRs of F19 were 98.88 ± 1.63% to HCT116 cells, 98.39 ± 2.29% to BGC823 cells, 77.43 ± 2.20% to SW1990 cells, and 37.32 ± 3.03% to CIK cells. At concentration of 0.5 μg/mL, IRs of F18 were 95.24 ± 5.14% to HCT116 cells, 87.68 ± 1.40% to BGC823 cells, 77.09 ± 3.13% to SW1990 cells, and 15.00 ± 1.48% to CIK cells; IRs of F19 were 95.63 ± 5.01% to HCT116 cells, 85.63 ± 5.01% to BGC823 cells, 68.91 ± 0.50% to SW1990 cells, and 22.99 ± 2.24% to CIK cells. Thus, in view of the high IR (≥70%) to tumor cells and low IR (< 50%) to CIK cells, we screened F18 and F19 as the HELT fractions.

3.3. Antitumor activity of lymphatic chemotherapy with HELT fraction emulsions in animal model

We used CRC lymphatic metastatic model to investigate the antitumor effect of HELT fraction *in vivo*. The animal model was established

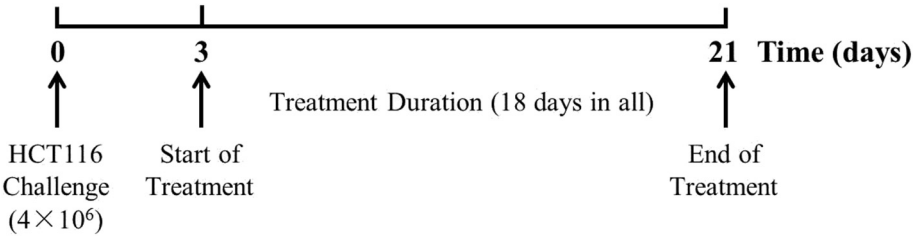

Fig. 3. The schedule of *in vivo* experiment. After establishing colorectal cancer lymphatic metastasis model based on injecting 4×10^6 of HCT116 cells into the right hind footpad of nude mice, the mice were treated with normal saline (NS), Cinobufacini Injection (CI), control emulsion (CE), low-dose emulsion (LD-E), middle-dose emulsion (MD-E), and high-dose emulsion (HD-E). The treatment duration was 18 days in all. The status of each mouse was assessed every 3 days.

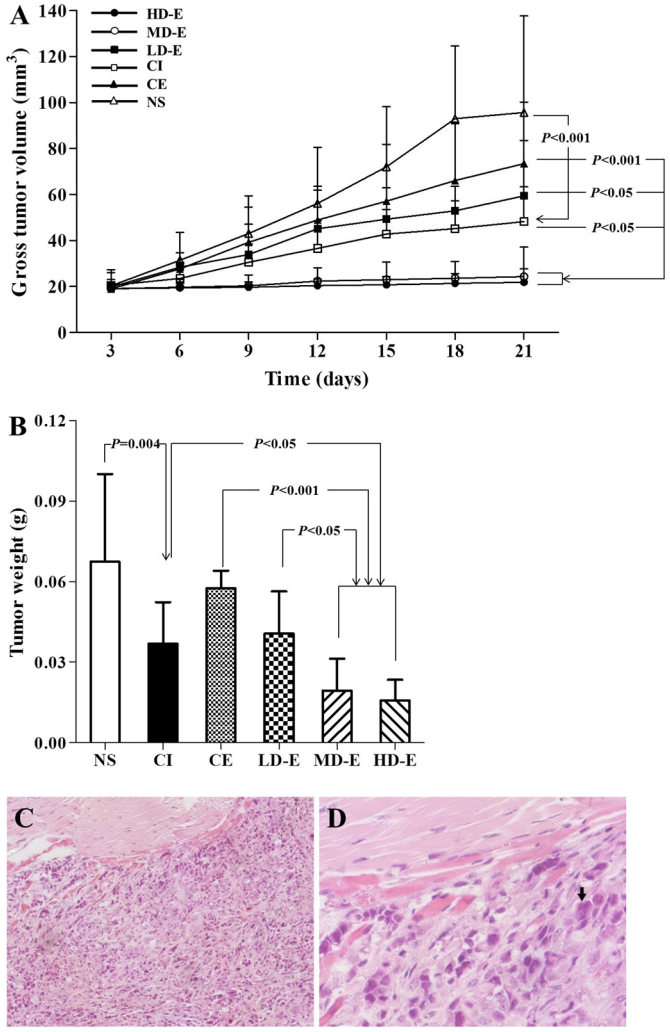

Fig. 4. *In vivo* antitumor effects of the HELT fraction. A. Tumor size was measured and gross tumor volume was calculated as (width^2 × length) / 2. The data are presented as the mean ± SD (n = 8). ANOVA analysis results indicated that tumor volume in the mice treated with HD-E and MD-E were significant smaller than that treated with LD-E ($P < 0.05$), CE ($P < 0.001$), and CI ($P < 0.05$), respectively. The tumor volume of CI group was significant smaller than NS group ($P < 0.001$). B. Tumor weight was measured at the end of treatment. The data are presented as the mean ± SD (n = 8). HD-E and MD-E produced significantly greater antitumor effects than LD-E ($P < 0.05$), CE ($P < 0.001$), and CI ($P < 0.05$), respectively. The tumor weight of CI group was significant smaller than NS group ($P = 0.004$). C and D. H&E staining of footpad tumor sections. C. ×100 magnification. D. ×400 magnification, black arrow presents a pathological mitotic figure. NS: normal saline; CI: Cinobufacini Injection; CE: control emulsion; LD-E: low-dose emulsion; MD-E: middle-dose emulsion; HD-E: high-dose emulsion.

by inoculating HCT116 cells into the right hind footpad of BALB/c nude mice. The *in-situ* tumor grew continuously into a palpable mass 3 days after tumor challenging and the tumor initiation rate was 100%. After that, the mice were divided into six groups and treated respectively as we described previously (Fig. 3).

During treatment, significant antitumor effects were witnessed in the group treated with HD-E and MD-E. HD-E and MD-E reduced tumor growth rate compared with LD-E, CI, and CE (Fig. 4A). Considering tumor weight, significant differences were found between HD-E (0.016 ± 0.008 g, n = 8), MD-E (0.019 ± 0.012 g, n = 8) group and LD-E (0.041 ± 0.016 g, n = 8), CE (0.058 ± 0.007 g, n = 8), CI (0.037 ± 0.016 g, n = 8) group, respectively (Fig. 4B). Although CI exhibited an antitumor activity comparing to NS (0.067 ± 0.033 g, n = 8), it was less effective than HD-E and MD-E ($P < 0.05$). The tumor IRs calculated by tumor weight were 72.6% in HD-E group, 66.24% in MD-E group, 29.37% in LD-E group, and 45.31% in CI group, respectively. H&E staining of tissue sections from the footpad tumors confirmed that the tumor cells infiltrated into the edge of the smooth muscle cells (Fig. 4C and D).

3.4. Inhibition of lymphatic metastasis by lymphatic chemotherapy

Abundant lymphatic vessels are located in the footpad of nude mouse, which form unidirectional lymphatic drainage. Thus, there exists a good anatomic basis of lymphatic metastasis and lymph chemotherapy. In our preliminary experiments, we injected Indian ink that could simulate and color lymph node into the footpad of nude mouse subcutaneously and found black colored lymph node located similar to the previous report [27]. Given the characteristics of lymphatic metastasis in CRC, we mainly observed the subiliac lymph node, medial iliac lymph node, and renal lymph node in the mouse.

After the 18-day treatment, we dissected the mice, counted the number of lymph node and confirmed the metastatic lymph node with H&E staining. The results indicated that HD-E and MD-E produced a significantly greater inhibition effect on LNM ($P < 0.05$) (Fig. 5). No difference was found between CI and NS. The concrete regional LNM rate of each group was shown in Table 2.

In addition, we also discovered the order and time of LNM. The HCT116 cells first move to subiliac lymph node, and then to medial iliac lymph node, finally to the renal lymph node. 5 days after inoculation, granule size of subiliac lymph node was palpated in each side of inguinal region (Fig. 6A) and another 5 days later, the metastatic ones were confirmed by H&E staining. At the end day of the experiment, 2 to 5 medial iliac lymph nodes were observed in iliac angiosomes (Fig. 6B) and 0 to 2 renal lymph nodes were observed in renal hilum after nephrectomy (Fig. 6C). However, the metastatic lymph node was only confirmed in minority of detected medial iliac lymph nodes. No renal lymph node metastasized was found until 6 weeks after inoculation. Histological analysis showed a massive tumor cells infiltrated within the lymph nodes (Fig. 6D and E).

3.5. The effects of HELT fraction emulsions on immune function

To assess the effects of F18 emulsions at different concentrations on immune function, we analyzed the SI value, NK cells and B cells. HD-E and MD-E promoted the proliferation of spleen cells as shown in Fig. 7. Moreover, the proportion of NK cells among peripheral blood was significantly higher in HD-E and MD-E group than others ($P < 0.01$,

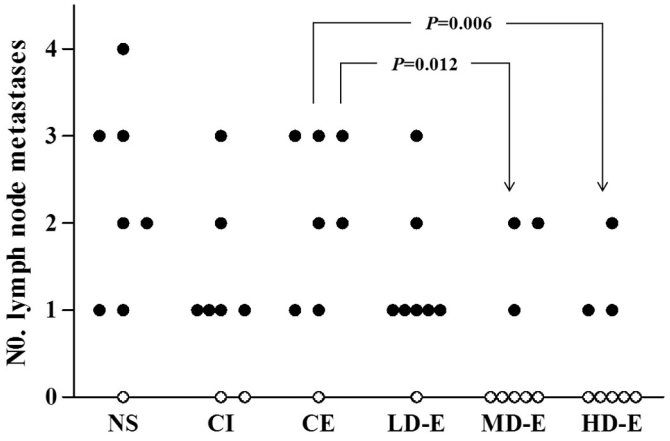

Fig. 5. Number of lymph node metastases per mouse of each group. Closed circles indicate one mouse with histologically-positive lymphatic metastasis. Opened circles indicate one mouse with histologically-negative lymphatic metastasis. The lymph node metastasis rate was significantly reduced in HD-E group ($P = 0.006$) and MD-E group ($P = 0.012$). NS: normal saline; CI: Cinobufacini Injection; CE: control emulsion; LD-E: low-dose emulsion; MD-E: middle-dose emulsion; HD-E: high-dose emulsion.

Table 2
Regional lymph node metastases in different groups.

Group	Subiliac ln. (m/d)	Medial iliac ln. (m/d)	Renal ln. (m/d)	Rate (%)
NS	10/16	6/25	0/13	29.65
CI	5/16	4/23	0/12	17.65
CE	10/16	5/21	0/13	30.00
LD-E	6/16	4/22	0/14	19.23
MD-E	4/16	1/19	0/16	9.80*
HD-E	2/16	2/19	0/13	8.33**

Ln.: lymph node; m/d: metastatic/detected; NS: normal saline; CI: Cinobufacini Injection; CE: control emulsion; LD-E: low-dose emulsion; MD-E: middle-dose emulsion; HD-E: high-dose emulsion.

* $P < 0.05$ *versus* control emulsion.

** $P < 0.01$ *versus* control emulsion.

Fig. 8A). The proportion of NK cells among spleen cells was also significantly higher in comparison of LD-E, CE, and NS group ($P < 0.05$, Fig. 8B). The proportion of B cells among peripheral blood and spleen cells was accordingly reduced.

To evaluate the secrete function of NK cells and B cells, the content

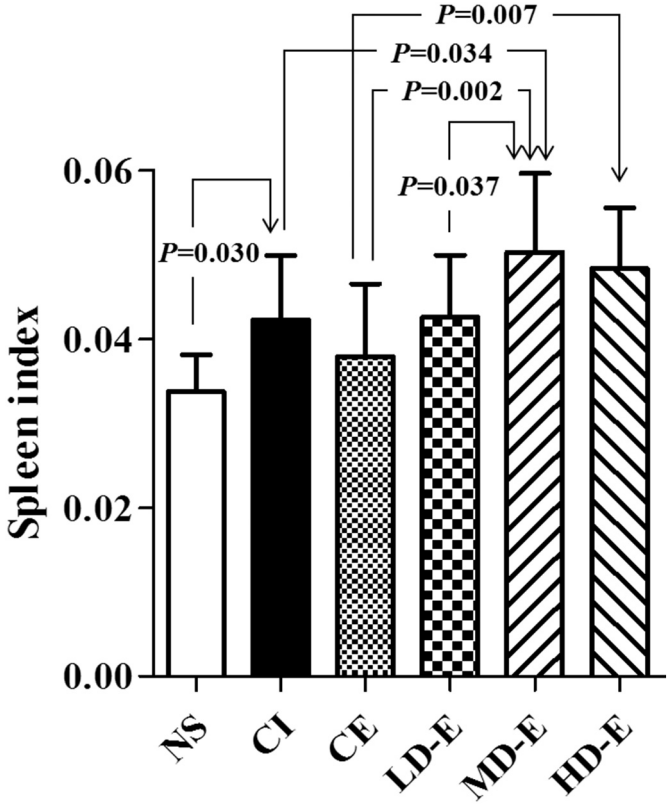

Fig. 7. The spleen index (SI) of each group. The spleen index was significantly higher in HD-E group ($P = 0.007$) and MD-E group ($P = 0.002$). NS: normal saline; CI: Cinobufacini Injection; CE: control emulsion; LD-E: low-dose emulsion; MD-E: middle-dose emulsion; HD-E: high-dose emulsion.

of IFN-γ and IgG1 in serum and the splenic cell supernatant were also respectively detected (Table 3). The results suggested that HD-E and MD-E significantly enhanced the secretion of IFN-γ in serum and the splenic cell supernatant as well as IgG1 in serum.

3.6. The potential toxicity of lymphatic chemotherapy with HELT fraction emulsions

We performed the hematological examination and evaluation of liver and renal function. As shown in Fig. 9, HD-E and MD-E

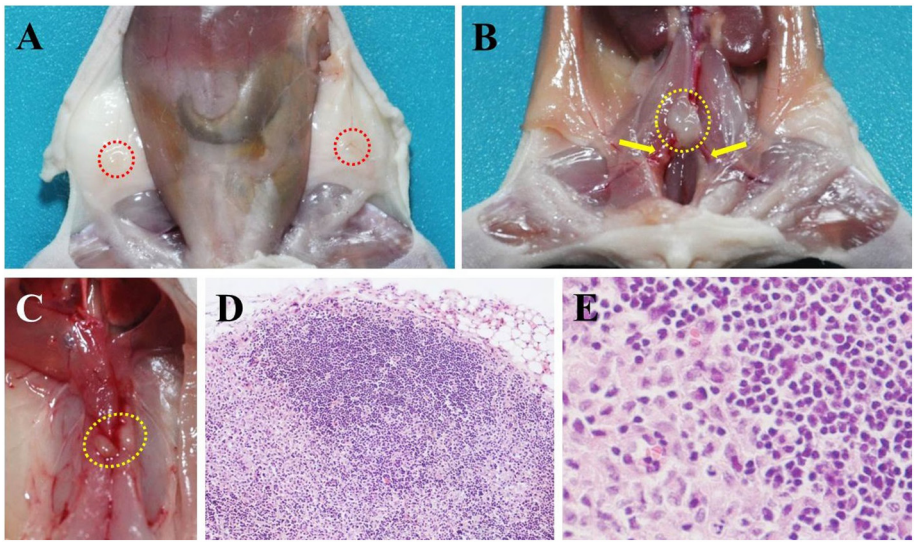

Fig. 6. Regional lymph nodes in mouse. A. Enlarged subiliac lymph nodes (red dotted circles) 5 days after tumor challenging. B. Enlarged medial iliac lymph nodes (yellow dotted circle) 21 days after tumor challenging and iliac vessels (yellow arrows). C. Renal lymph nodes (yellow dotted circles) 21 days after tumor challenging. D and E. H&E staining of metastasized lymph node sections showed numerous lymphocytes accumulating in lymph node. D. ×100 magnification. E. ×400 magnification. (For interpretation of the references to color in this figure legend, the reader is referred to the web version of this article.)

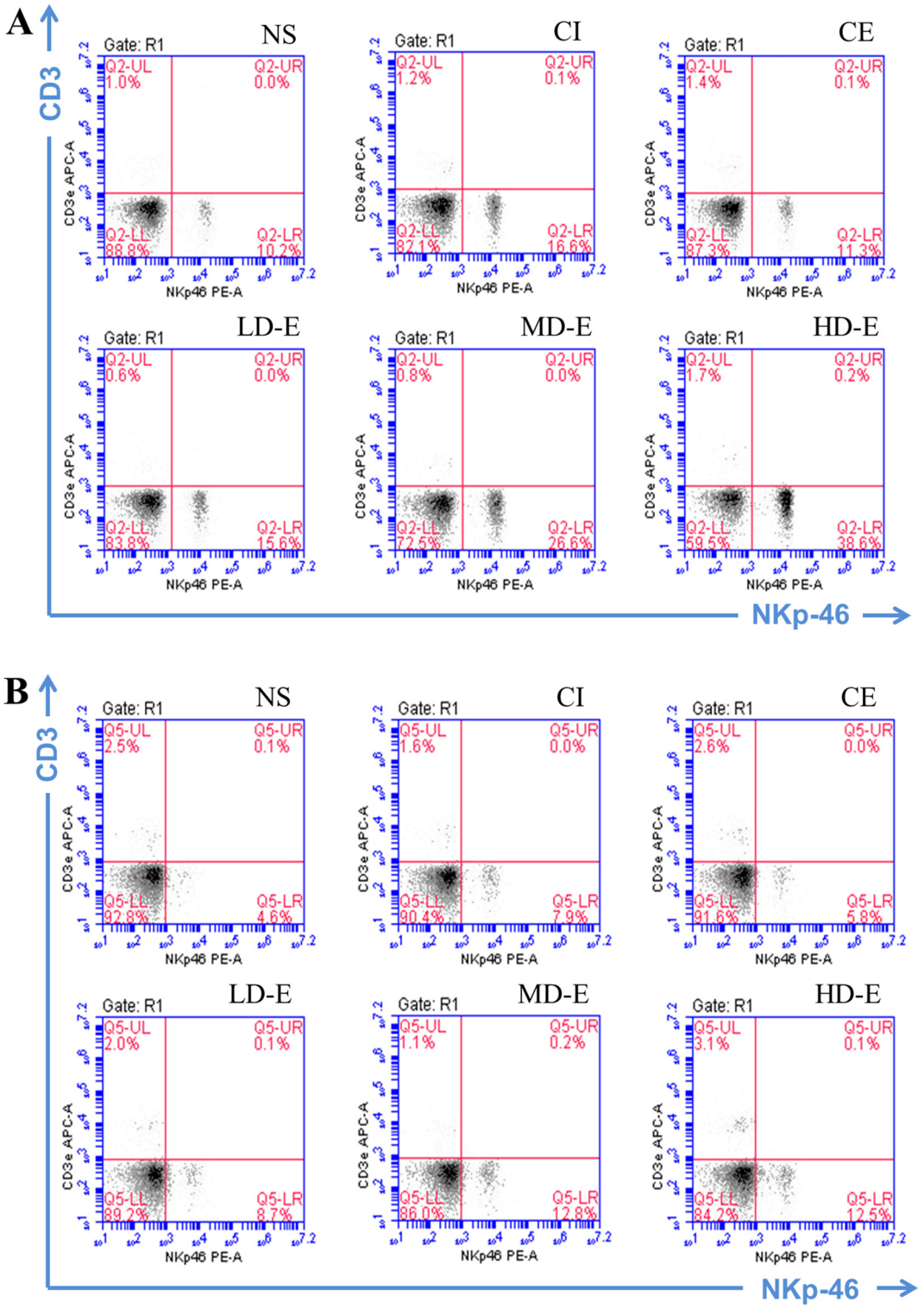

Fig. 8. The flow cytogram of NK cells among peripheral blood and spleen of each group. A. The proportion of NK cells among peripheral blood was significantly higher in HD-E and MD-E group than others ($P < 0.01$). B. The proportion of NK cells among spleen cells was also significantly higher in comparison of LD-E, CE, and NS group ($P < 0.05$). NS: normal saline; CI: Cinobufacini Injection; CE: control emulsion; LD-E: low-dose emulsion; MD-E: middle-dose emulsion; HD-E: high-dose emulsion.

significantly increased red blood cells, hemoglobin, white blood cells and platelet by activating hematopoietic function. In addition, HD-E and MD-E significantly increased the ratio of lymphocyte, meanwhile, reduced the ratio of neutrophil (Fig. 10A). However, the obvious side effects on liver function were also observed. The level of ALT and AST were significantly higher in HD-E group than other groups (Fig. 10B).

4. Discussion

Anti-cancer researches of traditional Chinese medicine (TCM) have been progressing greatly with the development and guidance of contemporary evidence-based medicine [14]. Constituent manufacture of TCM is vital for its modernization. Arteannuin and its derivation

Table 3
The content of IFN-γ and IgG1 in serum and the splenic cell supernatant.

Group	IFN-γ (ng/mL)		IgG1 (μg/mL)	
	Serum	Splenic cell supernatant	Serum	Splenic cell supernatant
NS	993.65 ± 62.15	1077.21 ± 119.18	68.18 ± 5.06	70.42 ± 6.42
CI	1217.30 ± 112.15	1242.00 ± 392.49	73.76 ± 6.97	73.93 ± 6.20
CE	1052.52 ± 63.56	1119.55 ± 123.02	70.65 ± 8.58	72.99 ± 6.22
LD-E	1083.82 ± 112.54	1155.90 ± 113.09	73.13 ± 2.23	75.64 ± 7.02
MD-E	1257.16 ± 166.19**	1587.65 ± 151.95**^	79.62 ± 5.88*	76.89 ± 5.94
HD-E	1303.28 ± 89.85**	1734.61 ± 65.60**^	79.87 ± 7.94*	77.92 ± 5.83

NS: normal saline; CI: Cinobufacini Injection; CE: control emulsion; LD-E: low-dose emulsion; MD-E: middle-dose emulsion; HD-E: high-dose emulsion.
* $P < 0.05$ *versus* CE.
** $P < 0.01$ *versus* CE.
^ $P < 0.05$ *versus* CI.

extracted from abrotanum are currently the most effective drugs to treat malaria, which is a successful case of constituent TCM [28]. In the first part of our study, we collected 22 fractions of bufadienolides separated and purified from the skin of *Bufo bufo gargarizans* Cantor (toad skin) based on the theory of constituent TCM. We haven't seen similar articles concerning such quantities of antitumor fractions of bufadienolides published domestically or internationally.

The skin of *Bufo bufo gargarizans* Cantor is a well-known TCM toad widely used in China. Toad skins consist of epidermis and dermis. The epidermis, exuviate of toad skins, possess little effective constituent, while the dermis containing venom gland and mucous gland is the essential constituent. CI (Cinobufacini Injection), also known as Huachansu, is the aqueous extract from the skins and parotid venom glands of *Bufo bufo gargarizans* Cantor. It has been officially approved

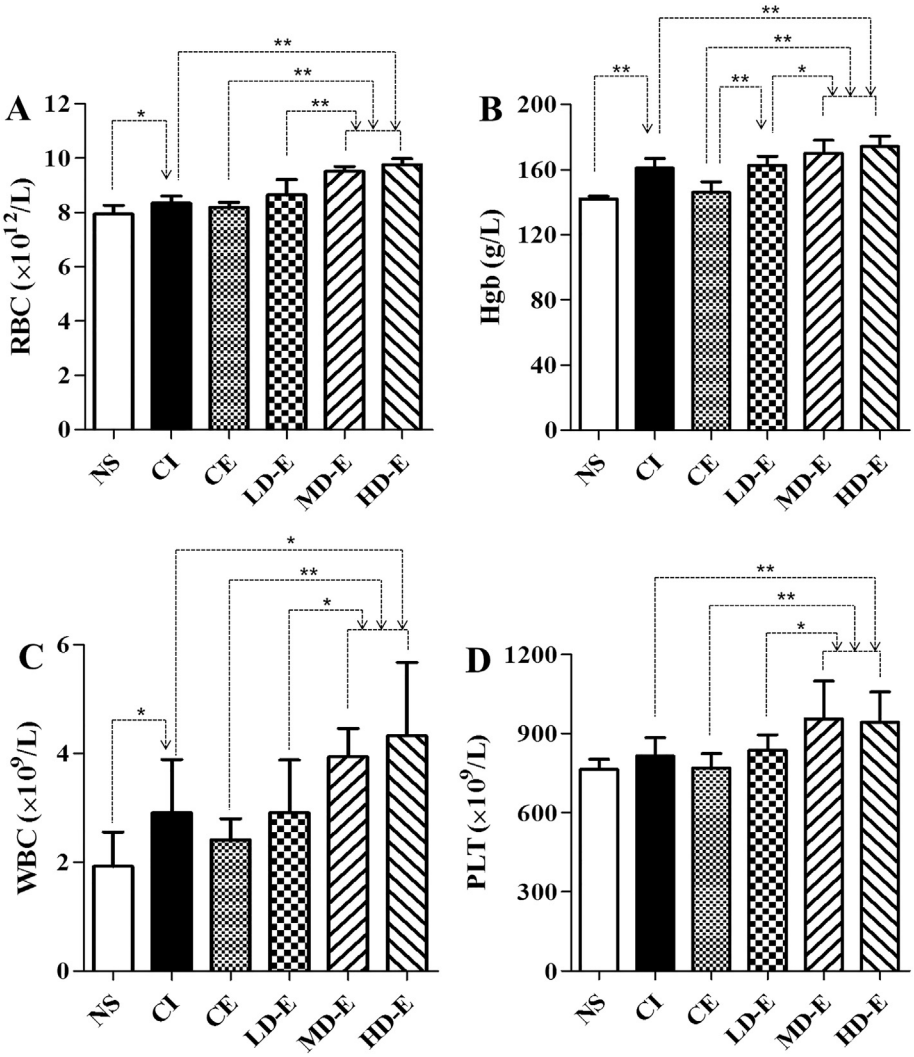

Fig. 9. The hematological examination of each group. A. HD-E and MD-E significantly increased red blood cells. B. HD-E and MD-E significantly increased hemoglobin. C. HD-E and MD-E significantly increased white blood cells. D. HD-E and MD-E significantly increased platelet. NS: normal saline; CI: Cinobufacini Injection; CE: control emulsion; LD-E: low-dose emulsion; MD-E: middle-dose emulsion; HD-E: high-dose emulsion.

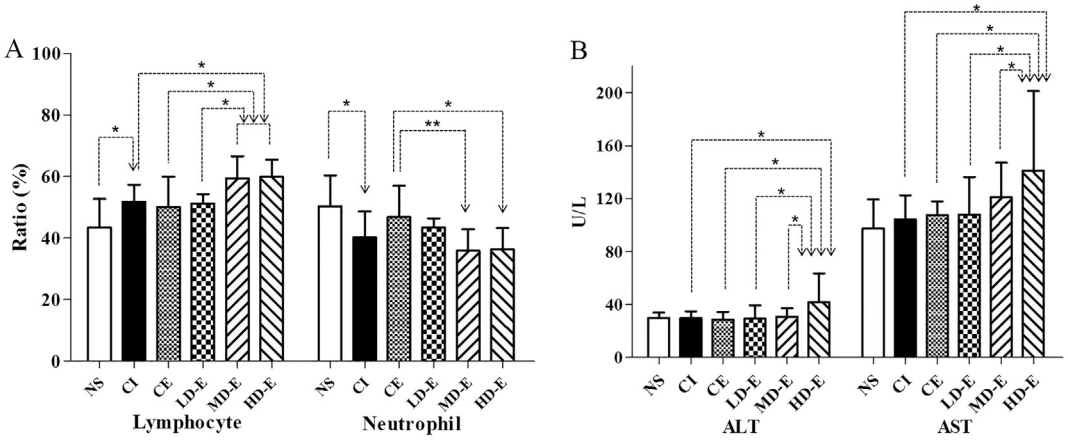

Fig. 10. The ratio of lymphocyte and neutrophil and the level of ALT and AST of each group. A. HD-E and MD-E significantly increased the ratio of lymphocyte and reduced the ratio of neutrophil. B. ALT and AST were significantly higher in HD-E group than other groups. NS: normal saline; CI: Cinobufacini Injection; CE: control emulsion; LD-E: low-dose emulsion; MD-E: middle-dose emulsion; HD-E: high-dose emulsion.

by the Chinese Food and Drug Administration since 1991 [29]. The antitumor mechanism of Cinobufacini includes inhibiting tumor cell proliferation, inducing differentiation and apoptosis, influencing autophagy-related genes expressing, EKR path, NA+-K+-ATPase and so on [30–34]. It may also alleviate paclitaxel-induced peripheral neuropathic pain and promote therapeutic efficacy of chemotherapy [33]. However, due to technical limitations, certain aqueous crude extract of toad exuviates applied in clinic have limited effects and serious adverse reactions [18]. It's known that the skins of toad *Bufo bufo gargarizans* Cantor is rich in bufadienolides, peptides and alkaloids [17]. Recently, bufadienolides have been shown to have the best antitumor activity with less adverse reaction for the treatment of liver and gastric cancers, compared to other components [35]. Bufadienolides, a C-24 steroid with a α-2-pyrone ring at its C-17 position, contain bufalin, cinobufagin, resibufogenin and telocinobufagin [17,36]. Previous studies showed that some fractions of bufadienolides such as resibufogenin have antitumor effect as well as toxicity and other side effects [17,18]. Our study aimed to screen constituents of bufadienolides with higher efficacy and lower toxicity and confirm its effects in lymphatic chemotherapy for CRC in a lymphatic metastatic model.

During the procedure of dissolving constituents, constituent 1–3 were totally dissolved in physiological saline and constituent 4–22 had to dissolve within DMSO. We found both inhibition effect and promotion effect in 22 constituents *in vitro*. The water-soluble constituent 1–3 and liposoluble constituent 21 and 22 had little antitumor effect and even promoted the growth of tumor cells. On the contrary, most of the liposoluble constituents, 4–20, obviously inhibited the tumor cells, especially the intermediate constituents such as 11. Meanwhile, CIK cells were inhibited by the intermediate constituents but were uninhibited or promoted by the ambilateral constituents. It thus indicated that both concentration and physical property of constituents were concerned with the effects on tumor cells and CIK cells. This result might explain why Cinobufacini, water-soluble medicament of toad skin, had limited antitumor effects and severe side effects in clinical practice.

According to *in vitro* ATP-TCA experiment, we screened two HELT constituents of bufadienolides namely F18 and F19 for further *in vivo* test. In recent years, lymphatic tract metastasis model has become a quite functional experiment tool in basic studies of cancer. There are profuse lymphatic tracts under pulvilli of nude mice and they can form monodirectional reflux including popliteal fossa, inguen, iliac blood vessel and renal hilus, eventually throughout the body. Wang L et al. has successfully established lymphatic tract metastasis model of breast cancer in nude mice by implanting MDA-MB-231 cells into mammary fat pads [26]. Long J et al. established a pancreatic cancer cell and mouse model with high lymphatic metastasis potential using BxPC-3-LN subline, derived from BxPC-3 human pancreatic cancer cell line. Researchers injected these BxPC-3 cells *via* footpads through serial passages in nude mice and found notable lymphatic metastasis was developed with 100% rate of success [37].

In the second part of our research, we applied F18 to prepare HELT anti-cancer ingredients emulsion and injected them into surroundings of pulvilli to assess its influence on both cancer cells and immune cells of BALB/c nude mice bearing HCT116 human colon adenocarcinoma cells. Results showed significantly higher inhibition effects on growth of xenograft tumors and LNM of group HD-E and MD-E compared to group LD-E and CI. Our research confirmed that HELT fraction F18 had antitumor effect and suggested that such effect was dose-dependent, which was in line with the findings of previous study [38]. Another point that should be mentioned was that Fig. 5 showed CI didn't significantly inhibit lymph node metastasis owing to several reasons: firstly, although Cinobufacini Injection had already been commercialized and applied clinically, the purity of active ingredient was still unclear; secondly, the difference between CI, NS, CE and LD-E might be small, for which the *P* value wasn't significant, yet we could notice a trend that inhibitory effect on LNM of CI and LD-E was similar and also higher than that of NS and CE; thirdly, as specification of CI showed, the pharmacological action of CI concerned three aspects including inhibiting tumor, promoting immunologic function and exerting antiviral effect, and water-solubility of CI might be the reason that drug density in lymph nodes was low for which anticancer effect wasn't noticeable.

Currently, drugs commonly used in clinical chemotherapy such as oxaliplatin, 5-fluorouracil have the ability of killing tumor cells effectively as well as inducing side effects and depressing the activity of immune cells [3]. It's crucial that ideal chemotherapeutics are found, maximizing the antineoplastic effect and minimizing the immunosuppressive influence. In our study, the SI value, the ratio of lymphocytes, the proportion of NK cells among peripheral blood and spleen, as well as the secretion of IFN-γ in NK cells and IgG1 in B lymphocytes of HD-E and MD-E were significantly higher compared with other groups, which indicated that HELT fraction of bufadienolides could stimulate immunologic function of nude mice, and thus might exert important influences on antitumor immunotherapy.

As for side effects, group MD-E, LD-E, CI and CE had no significant difference compared to NS group and only group HD-E had apparent influence on liver function. The results implied that liver injury caused by HD-E was mainly related to doses instead of emulsion type. In addition, emulsion could be applied as potential delivery system of chemotherapeutics in anticancer treatment with reduced toxicity [12].

Moreover, HD-E and MD-E significantly increased red blood cells, hemoglobin, white blood cells and platelet, which indicated that hemopoiesis function of marrow was distinctly promoted. The HELT constituent F18 is better than cinobufagin injection considering both influences on cancer cells and immunological function as well as other side effects.

Out of the purpose for drug development and synthesis, Dalian Institute of Chemical Physics conducted experiments screening active fractions of bufadienolides from toad skin [19] and kindly provided us those 22 fractions obtained through their study. Our researches mainly focus on pharmacodynamics experiments such as anticancer effects and side effects, as well as further clinical application. Finally, we screened two HELT constituents of bufadienolides namely F18 and F19. Specific composition of F18 or F19 needs further researches. By means of liquid chromatography-mass spectrometry (LC-MS) analysis, Dalian Institute of Chemical Physics has successfully identified several compounds in F13 [19]. In our pharmacodynamics study, F13 exerted significant antitumor functions as well as immunosuppressive effects. So far, among known compounds in F13, ψ-bufarenogin could notably restrain cancer through inhibiting EGFR and c-Met without obvious side effects [39]. In addition, ψ-bufarenogin could inhibit liver cancer stem cells (CSCs) through downregulating Sox2 expression [39]. Arenobufagin was capable of inhibiting cancer metastasis through regulating epithelial-mesenchymal transition (EMT) with decreasing expression of ZEB1, vimentin, and slug and increasing E-cadherin by targeting β-catenin [40]. Also, the author found that inhibition effect on EMT of Arenobufagin could be counteracted by overexpression of β-catenin while knocking down β-catenin strengthened this effect [40]. Telocinobufagin could significantly stimulate splenocyte proliferation, promote NK cells and macrophage activation, increase ratio of CD4+ and CD8+ cells among splenocytes, and what's more, Th1 cytokines such as IL1, IL12, IFN-γ and TNF-α were up-regulated while Th2 cytokines such as IL4 were down-regulated, which suggested that telocinobufagin could positively regulate immunologic function and might be clinically applied to treat cancer and immune-related diseases [41]. Cinobufotalin had strong antitumor effect and whether it's concerned with apoptosis remained inconsistent between different researches [42,43]. Heba Emam et al. revealed that Cinobufotalin could induce caspase-dependent apoptosis in U937, a human lymphoma cell, in which Fas played an important role, and moreover, using either Fas/FasL antagonist or pan-caspase inhibiter further verified their findings [43]. Besides, among other known constituents of bufadienolides, bufalin exerted prominent lethal effects on tumor cells and showed no obvious toxic side effects *in vivo* even though its concentration was as high as 0.4 mg/kg [44]. After treatment of bufalin, the researcher observed DNA condensation, decreased mitochondrial membrane potential and anti-apoptotic B-cell lymphoma 2 protein level, as well as increased reactive oxygen species, Fas/FasL, apoptosis protease activating factor 1, caspase 3/9, growth arrest- and DNA damage- inducible 153 gene expression. Further experiment *in vivo* verified anticancer effect of bufalin [44]. Cinobufagin could not only produce strong anti-tumor effects through inducing apoptosis and G1 phase arrest, but activate immunologic system like telocinobufagin [45,46]. Resibufogenin was able to inhibit cancer proliferation and metastasis through RIP3-mediated necroptosis, yet with some side cytotoxicity [47,48]. To summarize, we speculate that F18 and F19 are more likely to contain compounds with anticancer effects such as ψ-bufarenogin, Cinobufotalin and bufalin, as well as compounds with effects of motivating splenocyte proliferation and positively regulating immunologic functions such as telocinobufagin and cinobufagin. As for compounds with strong cytotoxicity such as resibufogenin, HELT fractions like F18 might have quite few or none contents like that. Nevertheless, experiments of HELT constituent F19 *in vitro* haven't been conducted yet and research about identification of exact compounds contained in F18 and F19 needs to be done further. What's more, specific mechanisms underlying HELT-induced anti-tumor and pro-immune effects remain undetermined and have yet to be investigated in the future.

In conclusion, the present study demonstrated the HELT constituents of bufadienolides exhibited high antitumor activity against three kinds of cancer cells and low toxicity to CIK cells. Moreover, we verified the effects of HELT constituent F18 on activating hematopoietic function, stimulating proliferation of the spleen and NK cells, and promoting the secretion of IFN-γ and IgG1 in a lymphatic metastatic model. These findings provide an experimental basis for clinical application of HELT bufadienolides in lymphatic chemotherapy.

Competing interests

The authors declared no conflicts of interests.

Acknowledgements

Funding

This work was supported by the National Natural Science Foundation of China, China (grant no. 81871317) and Beijing Lanhai Kangfu Medical Technology Research Co. Ltd.

Author contribution

Yingxin Xu, Shaoyou Xia and Xiaohui Du put forward the idea and designed the study. Zhenyu Zou, Shidong Hu, Zilong Hu and Yuxuan Li performed the experiments. Songyan Li, Hongliang Zhang, Yu Yang, Yichen Liu, Xiaolei Xu, Boyan Liu and Yufeng Wang participated in analyzing data. Changzheng He and Xiaowei Xing contributed to drafting the manuscript. All authors reviewed the manuscript.

References

[1] F. Bray, J. Ferlay, I. Soerjomataram, R.L. Siegel, L.A. Torre, A. Jemal, Global cancer statistics 2018: GLOBOCAN estimates of incidence and mortality worldwide for 36 cancers in 185 countries, CA Cancer J. Clin. 68 (6) (2018) 394–424, https://doi.org/10.3322/caac.21492.

[2] T.S. Kwon, S.B. Choi, Y.S. Lee, J.G. Kim, S.T. Oh, I.K. Lee, Novel methods of lymph node evaluation for predicting the prognosis of colorectal cancer patients with inadequate lymph node harvest, Cancer Res. Treat. 48 (1) (2016) 216–224, https://doi.org/10.4143/crt.2014.312.

[3] I. Depetris, D. Marino, A. Bonzano, C. Cagnazzo, R. Filippi, M. Aglietta, F. Leone, Fluoropyrimidine-induced cardiotoxicity, 124 (2018) (2018) 1–10, https://doi.org/10.1016/j.critrevonc.2018.02.002.

[4] J. Chen, Q. Yao, H. Wang, B. Wang, J. Zhang, T. Wang, Y. Lv, Z. Han, L. Wang, Lymphatic-targeted therapy following neoadjuvant chemotherapy: a promising strategy for lymph node-positive breast cancer treatment, Med. Oncol. 32 (7) (2015) 184, https://doi.org/10.1007/s12032-015-0634-7.

[5] H. Takeuchi, M. Ueda, T. Oyama, Y. Shimizu, Y. Kitagawa, Molecular diagnosis and translymphatic chemotherapy targeting sentinel lymph nodes of patients with early gastrointestinal cancers, Digestion 82 (3) (2010) 187–191, https://doi.org/10.1159/000309464.

[6] T. Oyama, H. Takeuchi, S. Matsuda, S. Ozawa, M. Kitajima, Y. Kitagawa, Translymphatic chemotherapy targeting sentinel lymph nodes using a novel phospholipid polymer-paclitaxel conjugate, Anticancer Res. 34 (4) (2014) 1751–1757.

[7] J. Liu, D. Meisner, E. Kwong, X.Y. Wu, M.R. Johnston, Translymphatic chemotherapy by intrapleural placement of gelatin sponge containing biodegradable paclitaxel colloids controls lymphatic metastasis in lung cancer, Cancer Res. 69 (3) (2009) 1174–1181, https://doi.org/10.1158/0008-5472.can-08-1753.

[8] X. Li, Q. Dong, Z. Yan, W. Lu, L. Feng, C. Xie, Z. Xie, B. Su, M. Liu, MPEG-DSPE polymeric micelle for translymphatic chemotherapy of lymph node metastasis, Int. J. Pharm. 487 (1–2) (2015) 8–16, https://doi.org/10.1016/j.ijpharm.2015.03.074.

[9] A.S. Mikhail, A.H. Negussie, W.F. Pritchard, D. Haemmerich, D. Woods, I. Bakhutashvili, J. Esparza-Trujillo, S.J. Brancato, J. Karanian, P.K. Agarwal, B.J. Wood, Lyso-thermosensitive liposomal doxorubicin for treatment of bladder cancer, Int. J. Hyperth. 33 (7) (2017) 733–740, https://doi.org/10.1080/02656736.2017.1315459.

[10] C.Y. Zhang, J. Gao, Z. Wang, Bioresponsive nanoparticles targeted to infectious microenvironments for sepsis management, Adv. Mater. 30 (43) (2018) e1803618, https://doi.org/10.1002/adma.201803618.

[11] J. Ye, Y. Liu, X. Xia, L. Meng, W. Dong, R. Wang, Z. Fu, H. Liu, R. Han, Improved safety and efficacy of a lipid emulsion loaded with a paclitaxel-cholesterol complex for the treatment of breast tumors, Oncol. Rep. 36 (1) (2016) 399–409, https://doi.org/10.3892/or.2016.4787.

[12] E. Dluska, A. Markowska-Radomska, A. Metera, B. Tudek, K. Kosicki, Multiple

emulsions as effective platforms for controlled anti-cancer drug delivery, Nanomedicine (Lond) 12 (18) (2017) 2183–2197, https://doi.org/10.2217/nnm-2017-0112.
[13] E.E. Frohlich, E. Frohlich, Cytotoxicity of nanoparticles contained in food on intestinal cells and the gut microbiota, Int. J. Mol. Sci. 17 (4) (2016) 509, https://doi.org/10.3390/ijms17040509.
[14] J. Liu, S. Wang, Y. Zhang, H.T. Fan, H.S. Lin, Traditional Chinese medicine and cancer: history, present situation, and development, Thorac Cancer 6 (5) (2015) 561–569, https://doi.org/10.1111/1759-7714.12270.
[15] H. Gao, R. Popescu, B. Kopp, Z. Wang, Bufadienolides and their antitumor activity, Nat. Prod. Rep. 28 (5) (2011) 953–969, https://doi.org/10.1039/c0np00032a.
[16] H. Emam, A. Refaat, P. Jawaid, M. Ur Rehman, P. Li, Q.L. Zhao, T. Kondo, Hyperthermia and radiation reduce the toxic side-effects of bufadienolides for cancer therapy, Oncol. Lett. 14 (1) (2017) 1035–1040, https://doi.org/10.3892/ol.2017.6256.
[17] F. Qi, A. Li, Y. Inagaki, N. Kokudo, S. Tamura, M. Nakata, W. Tang, Antitumor activity of extracts and compounds from the skin of the toad Bufo bufo gargarizans Cantor, Int. Immunopharmacol. 11 (3) (2011) 342–349, https://doi.org/10.1016/j.intimp.2010.12.007.
[18] Y. Xiao, Y.B. Zhao, Y.M. Xie, Experimental study of suspicious sensitization component screening on Huachansu injection, Zhongguo Zhong Yao Za Zhi 37 (18) (2012) 2824–2827.
[19] X. Li, Z. Guo, C. Wang, A. Shen, Y. Liu, X. Zhang, W. Zhao, X. Liang, Purification of bufadienolides from the skin of Bufo bufo gargarizans Cantor with positively charged C18 column, J. Pharm. Biomed. Anal. 92 (2014) 105–113, https://doi.org/10.1016/j.jpba.2014.01.002.
[20] X. Du, X. Wang, N. Ning, S. Xia, J. Liu, W. Liang, H. Sun, Y. Xu, Dynamic tracing of immune cells in an orthotopic gastric carcinoma mouse model using near-infrared fluorescence live imaging, Exp. Ther. Med. 4 (2) (2012) 221–225, https://doi.org/10.3892/etm.2012.579.
[21] P. Sun, Y. Xu, X. Du, N. Ning, H. Sun, W. Liang, R. Li, An engineered three-dimensional gastric tumor culture model for evaluating the antitumor activity of immune cells in vitro, Oncol. Lett. 5 (2) (2013) 489–494, https://doi.org/10.3892/ol.2012.1021.
[22] D.C. Li, X.K. Zhong, Z.P. Zeng, J.G. Jiang, L. Li, M.M. Zhao, X.Q. Yang, J. Chen, B.S. Zhang, Q.Z. Zhao, M.Y. Xie, H. Xiong, Z.Y. Deng, X.M. Zhang, S.Y. Xu, Y.X. Gao, Application of targeted drug delivery system in Chinese medicine, J. Control. Release 138 (2) (2009) 103–112, https://doi.org/10.1016/j.jconrel.2009.05.008.
[23] X.Y. Zhang, W.Y. Lu, Recent advances in lymphatic targeted drug delivery system for tumor metastasis, Cancer Biol Med 11 (4) (2014) 247–254, https://doi.org/10.7497/j.issn.2095-3941.2014.04.003.
[24] L.M. Dong Yan, Jiang Tong-ying, Qiu Dun-you, Liang Xin, Wang Si-ling, Preparation of Huachansu parenteral emulsion and studies on the quality of preparation, Journal of Shenyang Pharmaceutical University 26 (1) (2009) 6–10.
[25] X. Qi, L. Du, X. Chen, L. Chen, T. Yi, X. Chen, Y. Wen, Y. Wei, X. Zhao, VEGF-D-enhanced lymph node metastasis of ovarian cancer is reversed by vesicular stomatitis virus matrix protein, Int. J. Oncol. 49 (1) (2016) 123–132, https://doi.org/10.3892/ijo.2016.3527.
[26] L. Wang, C. Mi, W. Wang, Establishment of lymph node metastasis of MDA-MB-231 breast cancer model in nude mice, Zhonghua Yi Xue Za Zhi 95 (23) (2015) 1862–1865.
[27] C. Si, Y. Zhang, X. Lv, W. Yang, Z. Ran, P. Sun, In vivo lymph node mapping by Cadmium Tellurium quantum dots in rats, J. Surg. Res. 192 (2) (2014) 305–311, https://doi.org/10.1016/j.jss.2014.07.028.
[28] Z. Chang, The discovery of Qinghaosu (artemisinin) as an effective anti-malaria drug: a unique China story, Sci. China Life Sci. 59 (1) (2016) 81–88, https://doi.org/10.1007/s11427-015-4988-z.
[29] J. Qi, C.K. Tan, S.M. Hashimi, A.H. Zulfiker, D. Good, M.Q. Wei, Toad glandular secretions and skin extractions as anti-inflammatory and anticancer agents, Evid. Based Complement. Alternat. Med. 2014 (2014) 312684, , https://doi.org/10.1155/2014/312684.
[30] D. Chen, J. Chen, Y. Guo, Y. Li, Cinobufacini promotes apoptosis of bladder cancer cells by influencing the expression of autophagy-related genes, Oncol. Lett. 15 (5) (2018) 7104–7110, https://doi.org/10.3892/ol.2018.8206.
[31] J. Xia, Y. Inagaki, J. Gao, F. Qi, P. Song, G. Han, T. Sawakami, B. Gao, C. Luo, N. Kokudo, K. Hasegawa, Y. Sakamoto, W. Tang, Combination of cinobufacini and doxorubicin increases apoptosis of hepatocellular carcinoma cells through the Fas- and mitochondria-mediated pathways, Am. J. Chin. Med. 45 (7) (2017) 1537–1556, https://doi.org/10.1142/s0192415x17500835.
[32] Y. Jiang, L.S. Liu, L.P. Shen, Z.F. Han, H. Jian, J.X. Liu, L. Xu, H.G. Li, J.H. Tian, Z.J. Mao, Traditional Chinese Medicine treatment as maintenance therapy in advanced non-small-cell lung cancer: a randomized controlled trial, Complement. Ther. Med. 24 (2016) 55–62, https://doi.org/10.1016/j.ctim.2015.12.006.
[33] X. Ba, J. Wang, S. Zhou, X. Luo, Y. Peng, S. Yang, Y. Hao, G. Jin, Cinobufacini protects against paclitaxel-induced peripheral neuropathic pain and suppresses TRPV1 up-regulation and spinal astrocyte activation in rats, Biomed. Pharmacother. 108 (2018) 76–84, https://doi.org/10.1016/j.biopha.2018.09.018.
[34] L.Q. Sousa, K.D. Machado, S.F. Oliveira, L.D. Araujo, E.D. Moncao-Filho, A.A. Melo-Cavalcante, G.M. Vieira-Junior, P.M. Ferreira, Bufadienolides from amphibians: a promising source of anticancer prototypes for radical innovation, apoptosis triggering and Na(+)/K(+)-ATPase inhibition, Toxicon 127 (2017) 63–76, https://doi.org/10.1016/j.toxicon.2017.01.004.
[35] X. Wei, N. Si, Y. Zhang, H. Zhao, J. Yang, H. Wang, L. Wang, L. Han, B. Bian, Evaluation of bufadienolides as the main antitumor components in cinobufacin injection for liver and gastric cancer therapy, PLoS One 12 (1) (2017) e0169141, , https://doi.org/10.1371/journal.pone.0169141.
[36] X. Li, Y. Liu, A. Shen, C. Wang, J. Yan, W. Zhao, X. Liang, Efficient purification of active bufadienolides by a class separation method based on hydrophilic solid-phase extraction and reversed-phase high performance liquid chromatography, J. Pharm. Biomed. Anal. 97 (2014) 54–64, https://doi.org/10.1016/j.jpba.2014.04.015.
[37] J. Long, G. Luo, C. Liu, X. Cui, K. Satoh, Z. Xiao, B. Zhang, J. Xu, Q. Ni, M. Li, X. Yu, Development of a unique mouse model for pancreatic cancer lymphatic metastasis, Int. J. Oncol. 41 (5) (2012) 1662–1668, https://doi.org/10.3892/ijo.2012.1613.
[38] S. Lin, J. Lv, P. Peng, C. Cai, J. Deng, H. Deng, X. Li, X. Tang, Bufadienolides induce p53-mediated apoptosis in esophageal squamous cell carcinoma cells in vitro and in vivo, Oncol. Lett. 15 (2) (2018) 1566–1572, https://doi.org/10.3892/ol.2017.7457.
[39] J. Ding, H. Wang, psi-Bufarenogin, a lead compound of anti-cancer drug, vol. 14, (17) (2015) 2719–2720, https://doi.org/10.1080/15384101.2015.1071139.
[40] L. Chen, W. Mai, M. Chen, J. Hu, Z. Zhuo, X. Lei, L. Deng, J. Liu, N. Yao, M. Huang, Y. Peng, W. Ye, D. Zhang, Arenobufagin inhibits prostate cancer epithelial-mesenchymal transition and metastasis by down-regulating beta-catenin, Pharmacol. Res. 123 (2017) 130–142, https://doi.org/10.1016/j.phrs.2017.07.009.
[41] Y. Cao, Y. Song, N. An, S. Zeng, D. Wang, L. Yu, T. Zhu, T. Zhang, J. Cui, C. Zhou, X. Deng, The effects of telocinobufagin isolated from Chan Su on the activation and cytokine secretion of immunocytes in vitro, 23 (4) (2009) 457–464, https://doi.org/10.1111/j.1472-8206.2009.00696.x.
[42] S. Kai, J.H. Lu, P.P. Hui, H. Zhao, Pre-clinical evaluation of cinobufotalin as a potential anti-lung cancer agent, Biochem. Biophys. Res. Commun. 452 (3) (2014) 768–774, https://doi.org/10.1016/j.bbrc.2014.08.147.
[43] H. Emam, Q.L. Zhao, Y. Furusawa, A. Refaat, K. Ahmed, M. Kadowaki, T. Kondo, Apoptotic cell death by the novel natural compound, cinobufotalin, Chem. Biol. Interact. 199 (3) (2012) 154–160, https://doi.org/10.1016/j.cbi.2012.07.005.
[44] S.H. Wu, D.T. Bau, Y.T. Hsiao, K.W. Lu, T.C. Hsia, J.C. Lien, Y.C. Ko, W.H. Hsu, S.T. Yang, Y.P. Huang, J.G. Chung, Bufalin induces apoptosis in vitro and has antitumor activity against human lung cancer xenografts in vivo, Environ. Toxicol. 32 (4) (2017) 1305–1317, https://doi.org/10.1002/tox.22325.
[45] X.L. Wang, G.H. Zhao, J. Zhang, Q.Y. Shi, W.X. Guo, X.L. Tian, J.Z. Qiu, L.Z. Yin, X.M. Deng, Y. Song, Immunomodulatory effects of cinobufagin isolated from Chan Su on activation and cytokines secretion of immunocyte in vitro, J. Asian Nat. Prod. Res. 13 (5) (2011) 383–392, https://doi.org/10.1080/10286020.2011.565746.
[46] L. Zhu, Y. Chen, C. Wei, X. Yang, J. Cheng, Z. Yang, C. Chen, Z. Ji, Anti-proliferative and pro-apoptotic effects of cinobufagin on human breast cancer MCF-7 cells and its molecular mechanism, Nat. Prod. Res. 32 (4) (2018) 493–497, https://doi.org/10.1080/14786419.2017.1315575.
[47] Q. Han, Y. Ma, H. Wang, Y. Dai, C. Chen, Y. Liu, L. Jing, X. Sun, Resibufogenin suppresses colorectal cancer growth and metastasis through RIP3-mediated necroptosis, J. Transl. Med. 16 (1) (2018) 201, https://doi.org/10.1186/s12967-018-1580-x.
[48] J. Ning, Z.L. Yu, L.H. Hu, C. Wang, X.K. Huo, S. Deng, J. Hou, J.J. Wu, G.B. Ge, X.C. Ma, L. Yang, Characterization of phase I metabolism of resibufogenin and evaluation of the metabolic effects on its antitumor activity and toxicity, Drug Metab. Dispos. 43 (3) (2015) 299–308, https://doi.org/10.1124/dmd.114.060996.